HHS Public Access

Author manuscript

Arthritis Rheumatol. Author manuscript; available in PMC 2018 February 01.

Published in final edited form as:

Arthritis Rheumatol. 2017 February ; 69(2): 352–361. doi:10.1002/art.39844.

Deletion of Macrophage Migration Inhibitory Factor Reduces Severity of Osteoarthritis in Aged Mice

Meredith A. Rowe, PhD[1], **Lindsey R. Harper, BS**[2], **Margaret A. McNulty, PhD**[3], **Anthony G. Lau, PhD**[4], **Cathy S. Carlson, DVM, PhD**[2], **Lin Leng, PhD**[5], **Richard J. Bucala, MD, PhD**[5], **Richard A. Miller, MD, PhD**[6], and **Richard F. Loeser, MD**[1]

[1]Wake Forest School of Medicine, Winston-Salem, North Carolina and University of North Carolina at Chapel Hill, Chapel Hill, North Carolina.

[2]University of Minnesota, St. Paul, Minnesota.

[3]Louisiana State University, Baton Rouge, Louisiana.

[4]University of North Carolina at Chapel Hill, Chapel Hill, North Carolina.

[5]Yale University, New Haven, Connecticut.

[6]University of Michigan, Ann Arbor, Michigan.

Abstract

Objective—Macrophage migration inhibitory factor (MIF) is a pro-inflammatory cytokine that is elevated in the serum and synovial fluid of osteoarthritic (OA) patients. In this study, the potential role of MIF in OA was studied using human joint tissues and *in vivo* in mice with age-related and surgically induced OA.

Methods—MIF in conditioned media from human chondrocytes and meniscal cells and from cartilage explants was measured by ELISA. Severity of OA was analyzed histologically in male wild-type and *Mif*−/− mice at 12- and 22-months of age and following destabilization of the medial meniscus (DMM) surgery in 12-week old *Mif*−/− mice as well as in wild-type mice treated with a neutralizing MIF antibody. Synovial hyperplasia was graded in S100A8 immunostained histologic sections. Bone morphometric parameters were measured by microCT analysis.

Results—Human OA chondrocytes secreted 3-fold higher levels of MIF than normal chondrocytes, while normal and OA meniscal cells produced equivalent amounts. Compared to age- and strain-matched controls, the cartilage, bone, and synovium in older adult mice with *Mif* deletion were protected from changes of naturally occurring age-related OA. No protection from DMM-induced OA was seen in young adult *Mif*−/− mice or in wild-type mice treated with anti-MIF. Increased bone density in 8 week-old mice with *Mif* deletion was not maintained at 12-months.

Address correspondence to: Richard F. Loeser M.D., Thurston Arthritis Research Center, University of North Carolina, 3300 Thurston Building, CB #7280, Chapel Hill, NC 27599-7280. richard_loeser@med.unc.edu.

Conclusions—These results demonstrate a differential mechanism in the pathogenesis of naturally occurring age-related OA compared to injury-induced OA. The inhibition of MIF may represent a novel therapeutic target in the reduction of age-related OA.

Aging has been well-described as a key risk factor for the development of osteoarthritis (OA) (1). While aging does not directly cause OA, aging changes in joint tissues and possibly circulating factors that change with age increase the susceptibility for the development of the disease. Aging changes are reflected in the cartilage matrix including thinning of the articular cartilage (2) and the accumulation of advanced glycation end products (AGE) which alters the biomechanical properties of the joint (3). Aging changes are also evident in chondrocytes, where chondrocytes isolated from aged individuals are more resistant to stimulation with the growth factors insulin-like growth factor 1 (IGF-1) (4, 5), transforming growth factor-β (TGF-β) (6), and bone morphogenetic protein-6 (BMP-6) (7) than chondrocytes isolated from younger individuals. Inflammatory mediators have been found to be up-regulated in aged joint tissues including IL-7 in chondrocytes and synovial fluid in humans and IL-33, CXCL13, CCL8, and CCL5 in the mouse knee joint (reviewed in Greene and Loeser (8)). The increased expression of these inflammatory mediators, which is compounded by aging changes in the tissues, may contribute to the development of OA.

Macrophage migration inhibitory factor (MIF) is an inflammatory cytokine that has been studied for its role in the immune system. MIF has been shown to function as a cytokine that signals through the CD74 receptor (9) to increase neutrophil migration to regions of inflammation and to promote the innate immune response (10, 11). Additionally, MIF promotes macrophage activation, increasing phagocytosis and destruction of pathogens (11, 12). MIF has been studied in autoimmune diseases including rheumatoid arthritis (RA) and systemic lupus erythematosus (SLE). It has been shown to promote MMP-1 and MMP-3 production in synovial fibroblasts isolated from the knee joints of RA patients (13) and also has been shown to be significantly elevated in RA synovial fluid (14). In a more recent study, inhibition of MIF function either by deletion of *Mif,* or its receptor, *Cd74*, was found to reduce the severity of disease in an RA model by reducing both inflammation and bone erosion (15). In SLE, the amount of MIF in serum is positively correlated with tissue damage (16), and the renal expression of MIF was shown to be significantly elevated in an SLE-prone mouse model (17). The level of MIF was noted to be elevated in the serum and synovial fluid of patients with knee OA compared to healthy controls (14, 18). However, the potential contribution of MIF to the development of OA has not been previously studied.

Recently, *Mif*−/− 129Sv/C57Bl/6 mice were reported to have an increased lifespan when compared to wild-type (WT) controls, suggesting a role for MIF in the aging process (19), although more recent data (Miller, unpublished) suggest that this beneficial effect may be absent on other genetic backgrounds. Like OA, atherosclerosis is a common disease of aging and inhibition of MIF has been found to reduce atherosclerosis in a mouse model of the disease (20) suggesting that MIF may represent a therapeutic target for age-related disease. Given the association between aging and OA, we sought to determine the contribution of MIF to the development of OA. We found that genetic disruption of *Mif* decreased the severity of naturally-occurring OA in aged mice but not in a surgically-induced model of OA in younger adult mice.

MATERIALS & METHODS

Chondrocyte and meniscal cell isolation and culture

Normal human donor tissue (both knee and ankle joints) was obtained from the Gift of Hope Organ and Tissue Donor Network (Elmhurst IL) through the Rush University Medical Center in Chicago, IL. Osteoarthritic tissue was obtained as surgical waste from total knee replacement surgeries performed in the Department of Orthopaedic Surgery at Wake Forest Baptist Health and at the University of North Carolina Hospitals. The use of human tissue was approved by the Institutional Review Boards at Rush University, Wake Forest Baptist Health, and the University of North Carolina at Chapel Hill. All human donor tissue was de-identified before receipt, and the cartilage and meniscus were processed separately. The cartilage was dissected away from the subchondral bone in small flakes and rinsed in serum-free DMEM-F12 media (Gibco Life Technologies) to prevent the tissue from drying out. After the excess fat and ligamentous tissue were removed, the meniscus was dissected into small pieces to enable more efficient digestion. Cells were isolated separately from cartilage and meniscus using pronase and collagenase digestion as previously described (21). The cells were cultured in 10% serum DMEM-F12 media until confluent. Cultures were serum-starved overnight before media collection.

A 4mm biopsy punch was used to harvest human cartilage explants from the cartilage pieces that had been dissected away from the subchondral bone. Three explants per donor were pooled in one well and cultured in 10% serum DMEM-F12 media for approximately 72 hours. The explants were serum-starved for 48 hours before media collection. The explants were digested in papain, and the DNA content was quantified using the PicoGreen kit (Life Technologies) as previously described (22).

Experimental animals

The mice used for these studies were housed and maintained according to the IACUC guidelines at the respective institutions where each study was performed (The University of Michigan, Wake Forest School of Medicine, and The University of North Carolina at Chapel Hill). Knee joints from *Mif*−/− and wild-type (WT) mice for the aging experiment were from a previously reported study (19). For the surgically-induced OA studies, the *Mif*−/− colony was bred on the SV129/C57Bl/6 mixed background. The colony was maintained by heterozygous breeding, so the *Mif*−/− and WT mice used in these studies were age and strain-matched littermates. The C57Bl/6 mice used in the neutralizing antibody study were purchased directly from Jackson Labs.

ELISA

MIF content in serum-free conditioned media was quantified by solid-phase ELISA (R&D Systems) according to the manufacturer's protocol. Due to the high level of MIF in the media, the media samples were diluted 1:25 in the assay.

MIF immunostaining

Human normal and OA cartilage sections were a kind gift from Martin Lotz (Scripps Research Institute, La Jolla, CA). Human cartilage sections and mid-coronal sections from

12-month old wild-type and *Mif*−/− mouse knee joints were immunostained with anti-MIF (Life Technologies). Sections were de-paraffinized and rehydrated in serial ethanol washes followed by antigen retrieval in citrate buffer. Sections were first blocked with 3% H_2O_2 (Fisher Scientific) and then with Protein Block (Dako). The primary antibody was diluted in antibody diluent (Dako) and incubated on the sections overnight at 4°C. The following day, the sections were incubated with HRP-linked secondary antibody (Dako) and developed with the DAB chromagen (Dako). The sections were counterstained in Mayer's Hematoxylin (Sigma) and then dehydrated in serial ethanol washes.

DMM procedure

The destabilization of the medial meniscus (DMM) procedure was performed in 12-week old male *Mif*−/− and WT mice as described previously (23). This procedure induces OA by transecting the medial meniscotibial ligament (MMTL). For the sham surgery, the joint was opened and visualized, but the MMTL was not cut. We randomly assigned 14-16 mice to each surgical group and to each of the anti-MIF treatment and control groups (described below). The number of mice chosen for the present study was based on a power calculation using data from a previously published DMM and sham control experiment from our group that included 12-week old male C57BL/6 mice (23) and found that a sample size of 12 mice per group would provide greater than 80% power to detect at least a 50% difference in articular cartilage structure scores between groups. After the surgical procedure, the mice were monitored closely for signs of apparent pain or adverse effects of the procedure. The mice were maintained in normal housing conditions and allowed to exercise through normal activities. The mice were euthanized 10 weeks post-surgery, and the hind-limbs were collected in 10% formalin (Fisher Scientific) for histological analysis.

In the anti-MIF study, a neutralizing murine anti-MIF IgG1 (clone NIHIIID.9) and isotype control antibody were purified from ascites fluid using Protein A/G spin columns (Thermo Scientific). Following isolation, the antibodies were dialyzed overnight in DPBS (Lonza) and then filter-concentrated by centrifugation (Millipore). The antibody concentration was measured by the BCA assay (Thermo Scientific). After DMM surgery, mice were allowed to recover for five days before antibody treatment began. The antibodies were administered by IP injection for the duration of the study at a dose (20 mg/kg twice per week) previously shown to neutralize MIF in vivo (24). The mice were euthanized 10 weeks after surgery, and the legs were collected in formalin for histological analysis. Because repeated handling and injections can cause pain or other adverse effects which would be reflected with a decrease in food intake, the body weight of each mouse was monitored throughout the course of the study. All mice gained weight consistently over the course of the study, and there was no difference in the average body weights of each group at any time point during the study (data not shown).

Histology processing and OA grading

The formalin-fixed hind-limbs were transferred to 70% ethanol, and the excess soft tissue was removed. The samples were decalcified in 19% EDTA (Fisher Scientific), and the intact joints were embedded in paraffin. The joints were sectioned along the coronal plane at 4μm. Mid-coronal sections were stained with hematoxylin and eosin (H&E) and scored using the

articular cartilage structure (ACS) score developed by McNulty et al (25). This system scored the integrity of the articular cartilage on a scale of 0-12, where 0 represents normal healthy cartilage and 12 represents full-thickness loss of the articular cartilage across more than two-thirds of the surface scored. Adjacent mid-coronal sections were also stained with Safranin O and fast green and scored using the Saf-O score developed by McNulty et al (25). The Saf-O system scored the proteoglycan content of the articular cartilage on a scale of 0-12, where 0 represents uniform staining of healthy cartilage and 12 represents complete loss of staining across more than two-thirds of the surface. The Saf-O score is more sensitive to the mild to moderate lesions that result from the DMM procedure, as it relies on proteoglycan loss from the matrix vs. fibrillation and loss of cartilage. Therefore, it (rather than the ACS scoring system) was used to score OA in those studies. Additional joint measurements were made using the OsteoMeasure histomorphometry system (OsteoMetrics) as described (25). The additional parameters measured were: articular cartilage area and thickness, subchondral bone area and thickness, number of viable chondrocytes, area of chondrocyte necrosis, and calcified cartilage area and thickness.

Osteophyte assessment

Osteophytes were graded using a system that was modified from a previously published study (26). Osteophytes were graded on a scale of 0-3 as follows: 0 = no osteophyte, 1 = questionable/borderline osteophyte, 2 = small osteophyte, and 3 = large osteophyte. The summed osteophyte scores for the medial tibial plateau and the medial femoral condyle are presented.

Synovial assessment

Coronal sections were immunostained with anti-S100A8 (kindly provided by Johannes Roth) which has been used as a method to detect synovitis with synovial hyperplasia in mouse joints with OA (27). Immunohistochemistry was performed as above except that proteinase K was used for antigen retrieval. Synovial hyperplasia was graded on a single mid-coronal section from each mouse using a scale of 0-3 as follows: 0 = 1-3 cell layers in synovium, 1 = 4-6 cell layers, 2 = 7-9 cell layers, and 3 = 10 or more cell layers. The medial and lateral compartments of the joint were scored separately, and the sum of the two scores is presented.

MicroCT analysis

The knee joints from 8-week old (n=3 each *Mif*−/− and WT) and 12-month old (n=4 *Mif*−/− and n=5 WT) male mice were scanned with 10 μm resolution by microCT (μct80; Scanco Medical AG, Brüttisellen, Switzerland) as previously described (28). Bone morphometric parameters were measured in the trabecular bone of the proximal metaphysis of the tibia using Scanco software (Scanco Medical AG, Brüttisellen, Switzerland). The region of interest was consistently defined to begin inferior to the growth plate and extended for 1.00mm distally. Bone image data were rotated as necessary to adjust for any vertical alignments. The following histomorphometric trabecular bone parameters (29) were analyzed using the same threshold for each animal: bone volume fraction, tissue mineral density, connectivity density, trabecular number, trabecular separation, and trabecular thickness.

Statistical Analysis

All statistical analyses were performed using GraphPad Prism 6 with one exception: OA histomorphometry measurements were analyzed using SPSS, as noted. Data are presented graphically as individual data points with horizontal lines representing the mean of each group. MIF ELISA samples were collected from monolayer cultures of cells or explant cultures from unique human tissue donors (n=7-16 donors/group) and analyzed by unpaired t-test within each tissue type. OA severity (ACS and Saf-O scores) was analyzed from individual mice (n=13-16 mice/group) by Kruskal-Wallis nonparametric one-way ANOVA followed by Dunn's multiple comparisons test. Histomorphometric measurements were analyzed by heteroscedastic t-test. Synovial hyperplasia was evaluated in a subset of mice from the 12- and 22-month old groups (n=5-11 mice/group) and analyzed by Kruskal-Wallis nonparametric one-way ANOVA followed by Dunn's multiple comparisons test. Bone parameters were measured in individual mice (n=3-5 mice/group) and analyzed by two-way ANOVA followed by Tukey's multiple comparisons post-hoc test.

RESULTS

Human OA chondrocytes secrete higher levels of MIF than normal chondrocytes

Due to previously published results showing that MIF is present in higher levels in OA synovial fluid than in normal synovial fluid (14, 18), the amount of MIF secreted by joint tissue cells was measured to determine which tissues could be a source of MIF within the joint. Conditioned media samples were collected from unstimulated monolayer cultures of chondrocytes and meniscal cells and from unstimulated cartilage explant cultures, and the MIF protein level in the media was measured by ELISA (Fig. 1A and 1B). Chondrocytes isolated from OA cartilage secreted an average of 88.76±13.14ng/mL of MIF over 16 hours, which was significantly higher (p=0.0005) than that produced by chondrocytes from normal cartilage, which secreted an average of 28.23±7.78ng/mL of MIF. Cells from OA meniscus secreted an average of 47.62±11.73ng/mL of MIF, which was not significantly different from cells isolated from normal meniscus (31.65±5.54ng/mL). MIF in conditioned media from OA synovial fibroblasts was not detectable (data not shown).

OA cartilage explants released an average of 167.9±55.92pg MIF/ng DNA, which was significantly higher (p=0.0168) than that produced by normal cartilage explants, which released an average of 59.21±10.87pg MIF/ng DNA. MIF levels in human cartilage were visualized by immunostaining. MIF was localized to chondrocytes in sections from both normal (Fig. 1C) and OA donors (Fig. 1D) without significant differences in immunopositivity suggesting that the differences noted in cultured cells and explants were due to differences in MIF release into the media.

Mif deletion in mice reduces the severity of naturally occurring OA with age

In order to determine if MIF contributes to the development of OA *in vivo*, the stifle joints from 12-and 22-month old male *Mif*−/− and WT mice were analyzed for OA severity. Histological evaluation of hematoxylin and eosin (H&E) sections revealed characteristic OA changes in the joints of the WT mice at both ages, including degradation and loss of the articular cartilage, thickening of the subchondral bone, and osteophyte formation (Fig. 2A).

In contrast, the joints of the *Mif*−/− mice displayed more healthy appearing articular cartilage, normal thickness of the subchondral bone, and no osteophyte formation. Anti-MIF immunostaining in a WT section showed MIF expression in the meniscus and the articular cartilage (Fig. 2A). As expected, there was a lack of staining for MIF in the sections from *Mif*−/− mice.

OA severity in the 12- and 22-month old *Mif*−/− and WT mice, graded using the articular cartilage structure (ACS) score, revealed significantly higher ACS scores in the WT relative to the *Mif*−/− mice at both 12 and 22 months of age (Fig. 2B). WT mice at 12 and 22 months developed significantly larger osteophytes than the *Mif*−/− mice (Fig. 2C). The joints of the 12-and 22-month old *Mif*−/− and WT mice were further analyzed using histomorphometric analysis (Table 1). In both age groups, the *Mif*−/− mice maintained significantly greater articular cartilage area and thickness and more viable chondrocytes than the WT mice. Subchondral bone changes were also evident between the genotypes. The subchondral bone area and thickness were significantly greater in WT than in *Mif*−/− mice. The only two parameters which were not significantly different between *Mif*−/− and WT were the area of chondrocyte necrosis and the calcified cartilage area.

Synovitis with synovial hyperplasia is another characteristic of OA. S100A8 is an alarmin protein that is produced by synovial cells as well as activated macrophages and has been shown to correlate with synovitis (27, 30). Here, immunohistochemistry was performed using anti-S100A8 on coronal sections from 12- and 22-month old WT and *Mif*−/− mice (representative images are shown in Fig. 3A and 3B). In both genotypes, immunopositivity was evident throughout the joint – in the articular cartilage, the meniscus, and the synovium. Specifically in the WT joints, S100A8 immunopositivity was strong in both the cells and matrix of the synovium. As shown in Fig. 3A, S100A8 immunopositivity correlated with areas of synovial hyperplasia and thickening of the synovial lining. In contrast, the S100A8 synovial immunostaining results in the *Mif*−/− mice revealed minimal synovial hyperplasia. Based on the described synovial scoring system, there was no difference in the synovial hyperplasia between the 12-month old WT and *Mif*−/− mice, while the 22-month old WT mice exhibited more severe synovial hyperplasia than the *Mif*−/− mice (Fig. 3C). Additionally, the severity of synovial hyperplasia increased between 12 and 22 months in the WT mice.

Early bone differences in mice with *Mif* deletion are not maintained with age

Because of conflicting reports of bone density differences in *Mif*−/− mice compared to WT mice (31, 32) and the possibility that bone density differences could influence the development of OA (33), we measured trabecular bone parameters by μCT scans of the proximal metaphysis of the tibia from 8-week old and 12-month old male *Mif*−/− and WT mice. The 8-week old male *Mif*−/−mice had significantly greater bone volume fraction, tissue mineral density, and connectivity density than the age-matched WT mice. These differences were not maintained with age, as there were no significant differences in any bone parameters between 12-month old male *Mif*−/−and WT mice. Bone density parameters were also measured in female mice of the same ages, but there were no differences in these parameters between *Mif*−/− and WT mice in either age group (data not shown).

Mif deletion or treatment with a MIF neutralizing antibody does not reduce the severity of surgically-induced OA in young adult mice

We next wanted to determine if MIF was required for the development of surgically-induced OA in young adult mice. Here, we used the destabilization of the medial meniscus (DMM) surgical model to induce OA in 12-week old male *Mif*−/− and WT mice and evaluated the severity of cartilage lesions 10 weeks after surgery. Compared to the sham operated controls, both the WT and *Mif*−/− mice developed significant cartilage lesions; however, in contrast to the data on natural age-related OA, there was no difference in severity between the two groups (Fig. 5A). Both the WT and *Mif*−/− DMM mice developed significantly larger osteophytes than the sham mice, but there was no difference between the two groups (Fig 5B).

We also determined if inhibition of MIF systemically, using a neutralizing antibody, would alter the severity of surgically-induced OA. Twelve-week old male C57Bl/6 mice underwent the DMM procedure and were then treated for ten weeks with either a MIF neutralizing antibody or an IgG control antibody. The dose of anti-MIF used here was sufficient to inhibit MIF activity in a previous study (24). OA severity was analyzed ten weeks after surgery (Fig. 5C). Due to limitations in the amount of MIF antibody available and our previous data indicating that a sham control group did not develop OA changes, the contralateral legs were scored as the control group in this study. The DMM limbs of the control IgG-treated group and the anti-MIF-treated group developed significantly more severe OA than the contralateral limbs, and there was no difference in OA severity between the two treatment groups. The DMM limbs of both the IgG and MIF treatment groups developed significantly larger osteophytes than the contralateral limbs (Fig 5D).

DISCUSSION

Although OA is characterized by common pathologic changes within affected joints, the pathways that lead to OA can vary depending on the inciting factors. Here, we demonstrate that deletion of the pro-inflammatory cytokine MIF protects mice from developing naturally occurring age-related OA but not from developing injury-induced OA. These findings are in stark contrast to previous studies on mice with deletion of the pro-inflammatory cytokine IL-6 where age-related OA was more severe in the IL-6 knockouts (34) while they were protected from injury-induced OA using the same DMM model used in our MIF study (35). Other studies have also shown different effects when age-related and injury-induced OA were evaluated in mice with specific gene deletions including *Mmp3* which, similar to our results, had less age-related OA but no effects on OA severity in an injury model (reviewed in (36)). These studies emphasize the need to consider more than one model of OA when determining the role of a particular factor and indicate that the successful treatment of age-related OA and post-traumatic OA may require different targets.

The aged *Mif* knockouts not only exhibited less articular cartilage damage compared to age-matched wild types but also less synovial hyperplasia and fewer OA bone changes, including osteophytes. Synovial inflammation is evident in over 60% of clinical cases of OA as measured by MRI (37). Synovial inflammation is a key source of pain in OA due to macrophage infiltration and increased vascularization and innervation of the synovium (38).

We used the alarmin S100A8 as a marker of synovial changes due to its strong correlation with synovial hyperplasia and synovitis as well as its association with macrophage infiltration in the synovium (27, 30). However, while there is a clear correlation between the *Mif* genotype, synovial hyperplasia, and OA severity, it is difficult to determine if lack of MIF resulted in less synovial involvement and this contributed to cartilage protection or if less cartilage damage in the *Mif*−/−mice resulted in less synovial hyperplasia. The DMM model effectively induces OA changes in the cartilage and bone, but minimal synovitis has been observed in this model (39). We also did not observe significant synovitis or synovial hyperplasia in our DMM mice (data not shown) suggesting that the differential effect of *Mif* knockout on age-related OA and DMM-induced OA may be due to a differential role of the synovium. This would be consistent with studies that have shown that MIF contributes to synovitis in models of inflammatory arthritis (40). As MIF is constitutively expressed in the joint, it is possible that it exerts an age-related deleterious action on joint homeostasis but is not important in the acute setting of joint injury when the expression of other inflammatory mediators prevail.

The finding that the ACS scores in the wild-type mice did not change significantly between 12- and 22-months was unexpected. Since this was a cross-sectional study it is not possible to determine if this was due to a lack of progression of the cartilage changes or just a chance occurrence in two different sets of mice. However, we did note that there was a significant decrease in the subchondral bone area between the 12- and 22-month old WT mice, and there was a trend towards a significant decrease in the articular cartilage area between the two groups, but we did not note differences in the number of viable chondrocytes or in the area of chondrocyte necrosis. These aging changes in the mice are similar to aging changes in humans where there is a thinning of the articular cartilage (2), a decrease in the number of viable chondrocytes (41), and an overall increase in bone turnover (1).

There is some controversy over the role of MIF in bone. Studies have shown that MIF inhibits osteoclastogenesis through activation of the tyrosine kinase Lyn (42), and that *Mif*−/−mice have significantly less bone volume than WT mice (32). Alternatively, MIF has been shown to be necessary for osteoclastogenesis in a mouse model of rheumatoid arthritis and *Mif*−/−mice were protected from development of bone erosions in this model (15). Because increased bone density has been shown to be a potential risk factor for incident OA while increased bone turnover may promote progression (43, 44), we examined bone density in young and older adult *Mif*−/− mice. We found that the BV/TV and other bone parameters were higher in young *Mif*−/−mice compared to WT mice, but these early bone differences were not maintained with age. Therefore, it is unlikely that these early bone density differences were responsible for the reduced OA severity seen in the older adult *Mif*−/− mice.

It is not clear from the present study if *Mif* deletion had a direct effect on the articular chondrocytes that could explain less severe age-related OA. Immunohistochemistry results revealed that chondrocytes, as well as meniscal cells, were immunopositive for MIF and released MIF into the media when cultured. Similar intracellular staining and release has been seen with other cell types such as macrophages (12) and RA synovial fibroblasts (14). Chondrocytes, but not meniscal cells, from OA joints secreted more MIF than cells from

normal joints. However, we could not detect an effect of extracellular MIF on joint tissue cells. We performed a series of *in vitro* studies using recombinant MIF in doses up to 1 μg/mL and could not detect an increase in ERK, p38, or JNK MAP kinase activation or increase in MMP production in cultures of human chondrocytes, meniscal cells, or synovial fibroblasts (supplemental Fig.1).

These *in vitro* results with joint tissue cells are contrary to published studies with other cell types that reported recombinant MIF-stimulated phosphorylation of the ERK MAP kinase in Raji cells (a B cell line) (9) and in primary rat osteoblasts (45). Additional published studies show recombinant MIF-stimulated production of MMP-1 and MMP-3 production in synovial fibroblasts isolated from OA and RA patients (13) as well as MMP-9 and MMP-13 production in primary rat osteoblasts (45). However, those studies required doses of MIF up to 10 μg/mL to detect a response that far exceeds the amount of MIF measured in synovial fluid, which ranges from 3 to 19 ng/mL (14, 18), or the amount of MIF we measured in conditioned media from confluent chondrocyte and meniscal cell monolayers, which ranged from 1 to 140 ng/ml. We examined chondrocytes for the presence of CD74, which is the primary receptor for MIF, but could not detect significant levels on the cell surface by flow cytometry (unpublished results). These findings suggest that chondrocytes produce and secrete MIF but that it does not have an autocrine effect on cartilage. MIF may instead promote OA by promoting macrophage infiltration into the joint, which would explain the reduced synovial hyperplasia observed in the aged mice with MIF deleted. MIF also has been described to exert intracellular functions by intracytoplasmic interaction with the COP9 signalosome that influences cell cycle progression (46). Accordingly, the distinction we observed between the effects *Mif* deletion versus immunoneutralization may be accounted for by a strictly intracellular role for MIF in chondrocytes.

Taken together, the results presented here indicate that the lack of MIF has a strong protective effect on naturally occurring age-related OA. As the percentage of adults over the age of 65 continues to increase, the prevalence of aging-related diseases, including OA, is also increasing (47). MIF is encoded in a functionally polymorphic locus that occurs commonly in the population (48), and our data prompt investigation into the potential role of variant *MIF* alleles in OA incidence or progression. Therapies that are able to stop or slow the progression of diseases of aging are necessary in order to improve the quality of life and to extend the healthy lifespan of the aging population.

Supplementary Material

Refer to Web version on PubMed Central for supplementary material.

ACKNOWLEDGEMENTS

We thank the Gift of Hope Tissue and Organ Donor Network, Dr. Susan Chubinskaya, and the donor families for providing normal donor tissue. We also thank the Department of Orthopaedic Surgery at Wake Forest Baptist Health and the University of North Carolina for providing osteoarthritic tissue. We thank Dr. Tom Smith (Department of Orthopaedic Surgery, Wake Forest School of Medicine) and Kathryn Kelley (Thurston Arthritis Research Center, University of North Carolina at Chapel Hill) for their assistance in performing the DMM surgeries as well as Melissa Roy, Dr. Alexandra Armstrong, and Dr. Laura Pritzker (University of Minnesota) for their assistance with histological grading/morphometry and Dr. Ted Bateman and Eric Livingston (University of North Carolina at Chapel Hill) for their assistance with the microCT. We also thank Dr. Martin Lotz (Scripps Research

Institute, La Jolla, CA) for his kind gift of the human cartilage sections, Dr. Peter van der Kraan (Radboud University Medical Center, Nijmegen) for his advice regarding our synovial studies, and Dr. Johannes Roth (Institute of Immunology, University of Münster, Münster) for his kind gift of the S100A8 antibody.

This work was supported by grants from the National Institute on Aging (AG046990) to M.A.R., (AG044185) to R.F.L., and (AG024824) to R.A.M. and from the National Institute of Arthritis and Musculoskeletal and Skin Diseases (AR049610) to R.J.B.

REFERENCES

1. Loeser RF. Age-related changes in the musculoskeletal system and the development of osteoarthritis. Clin Geriatr Med. 2010; 26:371–386. [PubMed: 20699160]
2. Ding C, Cicuttini F, Scott F, Cooley H, Jones G. Association between age and knee structural change: a cross sectional MRI based study. Ann Rheum Dis. 2005; 64:549–555. [PubMed: 15769915]
3. Chen AC, Temple MM, Ng DM, Verzijl N, DeGroot J, TeKoppele JM, et al. Induction of advanced glycation end products and alterations of the tensile properties of articular cartilage. Arthritis Rheumatol. 2002; 46:3212–3217.
4. Loeser RF, Gandhi U, Long DL, Yin W, Chubinskaya S. Aging and oxidative stress reduce the response of human articular chondrocytes to insulin-like growth factor 1 and osteogenic protein 1. Arthritis Rheumatol. 2014; 66:2201–2209. [PubMed: 24664641]
5. Messai H, Duchossoy Y, Khatib AM, Panasyuk A, Mitrovic DR. Articular chondrocytes from aging rats respond poorly to insulin-like growth factor-1: an altered signaling pathway. Mech Ageing Dev. 2000; 115:21–37. [PubMed: 10854627]
6. Blaney Davidson EN, Scharstuhl A, Vitters EL, van der Kraan PM, van den Berg WB. Reduced transforming growth factor-beta signaling in cartilage of old mice: role in impaired repair capacity. Arthritis Res Ther. 2005; 7:R1338–1347. [PubMed: 16277687]
7. Bobacz K, Gruber R, Soleiman A, Erlacher L, Smolen JS, Graninger WB. Expression of bone morphogenetic protein 6 in healthy and osteoarthritic human articular chondrocytes and stimulation of matrix synthesis in vitro. Arthritis Rheumatol. 2003; 48:2501–2508.
8. Greene MA, Loeser RF. Aging-related inflammation in osteoarthritis. Osteoarthritis Cartilage. 2015; 23:1966–1971. [PubMed: 26521742]
9. Leng L, Metz CN, Fang Y, Xu J, Donnelly S, Baugh J, et al. MIF signal transduction initiated by binding to CD74. J Exp Med. 2003; 197:1467–1476. [PubMed: 12782713]
10. Rajasekaran D, Zierow S, Syed M, Bucala R, Bhandari V, Lolis EJ. Targeting distinct tautomerase sites of D-DT and MIF with a single molecule for inhibition of neutrophil lung recruitment. FASEB J. 2014; 28:4961–4971. [PubMed: 25016026]
11. Mitchell RA, Liao H, Chesney J, Fingerle-Rowson G, Baugh J, David J, et al. Macrophage migration inhibitory factor (MIF) sustains macrophage proinflammatory function by inhibiting p53: regulatory role in the innate immune response. Proc Natl Acad Sci U S A. 2002; 99:345–350. [PubMed: 11756671]
12. Calandra T, Bernhagen J, Mitchell RA, Bucala R. The macrophage is an important and previously unrecognized source of macrophage migration inhibitory factor. J Exp Med. 1994; 179:1895–1902. [PubMed: 8195715]
13. Onodera S, Kaneda K, Mizue Y, Koyama Y, Fujinaga M, Nishihira J. Macrophage migration inhibitory factor up-regulates expression of matrix metalloproteinases in synovial fibroblasts of rheumatoid arthritis. J Biol Chem. 2000; 275:444–450. [PubMed: 10617637]
14. Onodera S, Tanji H, Suzuki K, Kaneda K, Mizue Y, Sagawa A, et al. High expression of macrophage migration inhibitory factor in the synovial tissues of rheumatoid joints. Cytokine. 1999; 11:163–167. [PubMed: 10089139]
15. Gu R, Santos LL, Ngo D, Fan H, Singh PP, Fingerle-Rowson G, et al. Macrophage migration inhibitory factor is essential for osteoclastogenic mechanisms in vitro and in vivo mouse model of arthritis. Cytokine. 2015; 72:135–145. [PubMed: 25647268]
16. Foote A, Briganti EM, Kipen Y, Santos L, Leech M, Morand EF. Macrophage migration inhibitory factor in systemic lupus erythematosus. J Rheumatol. 2004; 31:268–273. [PubMed: 14760795]

17. Hoi AY, Hickey MJ, Hall P, Yamana J, O'Sullivan KM, Santos LL, et al. Macrophage migration inhibitory factor deficiency attenuates macrophage recruitment, glomerulonephritis, and lethality in MRL/lpr mice. J Immunol. 2006; 177:5687–5696. [PubMed: 17015758]
18. Liu M, Hu C. Association of MIF in serum and synovial fluid with severity of knee osteoarthritis. Clin Biochem. 2012; 45:737–739. [PubMed: 22449335]
19. Harper JM, Wilkinson JE, Miller RA. Macrophage migration inhibitory factor-knockout mice are long lived and respond to caloric restriction. FASEB J. 2010; 24:2436–2442. [PubMed: 20219983]
20. Bernhagen J, Krohn R, Lue H, Gregory JL, Zernecke A, Koenen RR, et al. MIF is a noncognate ligand of CXC chemokine receptors in inflammatory and atherogenic cell recruitment. Nat Med. 2007; 13:587–596. [PubMed: 17435771]
21. Loeser RF, Pacione CA, Chubinskaya S. The combination of insulin-like growth factor 1 and osteogenic protein 1 promotes increased survival of and matrix synthesis by normal and osteoarthritic human articular chondrocytes. Arthritis Rheumatol. 2003; 48:2188–2196.
22. Yin W, Park JI, Loeser RF. Oxidative stress inhibits insulin-like growth factor-I induction of chondrocyte proteoglycan synthesis through differential regulation of phosphatidylinositol 3-Kinase-Akt and MEK-ERK MAPK signaling pathways. J Biol Chem. 2009; 284:31972–31981. [PubMed: 19762915]
23. Loeser RF, Olex AL, McNulty MA, Carlson CS, Callahan MF, Ferguson CM, et al. Microarray analysis reveals age-related differences in gene expression during the development of osteoarthritis in mice. Arthritis Rheumatol. 2012; 64:705–717.
24. Leng L, Chen L, Fan J, Greven D, Arjona A, Du X, et al. A small-molecule macrophage migration inhibitory factor antagonist protects against glomerulonephritis in lupus-prone NZB/NZW F1 and MRL/lpr mice. J Immunol. 2011; 186:527–538. [PubMed: 21106847]
25. McNulty MA, Loeser RF, Davey C, Callahan MF, Ferguson CM, Carlson CS. A comprehensive histological assessment of osteoarthritis lesions in mice. Cartilage. 2011; 2:354–363. [PubMed: 26069594]
26. Miller RE, Tran PB, Das R, Ghoreishi-Haack N, Ren D, Miller RJ, et al. CCR2 chemokine receptor signaling mediates pain in experimental osteoarthritis. Proc Natl Acad Sci U S A. 2012; 109:20602–20607. [PubMed: 23185004]
27. Schelbergen RF, de Munter W, van den Bosch MH, Lafeber FP, Sloetjes A, Vogl T, et al. Alarmins S100A8/S100A9 aggravate osteophyte formation in experimental osteoarthritis and predict osteophyte progression in early human symptomatic osteoarthritis. Ann Rheum Dis. 2014; 75:218–225. [PubMed: 25180294]
28. Lau AG, Sun J, Hannah WB, Livingston EW, Heymann D, Bateman TA, et al. Joint bleeding in factor VIII deficient mice causes an acute loss of trabecular bone and calcification of joint soft tissues which is prevented with aggressive factor replacement. Haemophilia. 2014; 20:716–722. [PubMed: 24712867]
29. Muller R, Van Campenhout H, Van Damme B, Van Der Perre G, Dequeker J, Hildebrand T, et al. Morphometric analysis of human bone biopsies: a quantitative structural comparison of histological sections and micro-computed tomography. Bone. 1998; 23:59–66. [PubMed: 9662131]
30. Schelbergen RF, van Dalen S, ter Huurne M, Roth J, Vogl T, Noel D, et al. Treatment efficacy of adipose-derived stem cells in experimental osteoarthritis is driven by high synovial activation and reflected by S100A8/A9 serum levels. Osteoarthritis Cartilage. 2014; 22:1158–1166. [PubMed: 24928317]
31. Oshima S, Onodera S, Amizuka N, Li M, Irie K, Watanabe S, et al. Macrophage migration inhibitory factor-deficient mice are resistant to ovariectomy-induced bone loss. FEBS Lett. 2006; 580:1251–1256. [PubMed: 16442103]
32. Jacquin C, Koczon-Jaremko B, Aguila HL, Leng L, Bucala R, Kuchel GA, et al. Macrophage migration inhibitory factor inhibits osteoclastogenesis. Bone. 2009; 45:640–649. [PubMed: 19591967]
33. Hardcastle SA, Dieppe P, Gregson CL, Davey Smith G, Tobias JH. Osteoarthritis and bone mineral density: are strong bones bad for joints? Bonekey Rep. 2015; 4:624. [PubMed: 25628884]

34. de Hooge AS, van de Loo FA, Bennink MB, Arntz OJ, de Hooge P, van den Berg WB. Male IL-6 gene knock out mice developed more advanced osteoarthritis upon aging. Osteoarthritis Cartilage. 2005; 13:66–73. [PubMed: 15639639]
35. Ryu JH, Yang S, Shin Y, Rhee J, Chun CH, Chun JS. Interleukin-6 plays an essential role in hypoxia-inducible factor 2alpha-induced experimental osteoarthritic cartilage destruction in mice. Arthritis Rheumatol. 2011; 63:2732–2743.
36. Little CB, Zaki S. What constitutes an "animal model of osteoarthritis"--the need for consensus? Osteoarthritis Cartilage. 2012; 20:261–267. [PubMed: 22321719]
37. Wang X, Jin X, Han W, Cao Y, Halliday A, Blizzard L, et al. Cross-sectional and longitudinal associations between knee joint effusion synovitis and knee pain in older adults. J Rheumatol. 2015; 43:121–130. [PubMed: 26568597]
38. Benito MJ, Veale DJ, FitzGerald O, van den Berg WB, Bresnihan B. Synovial tissue inflammation in early and late osteoarthritis. Ann Rheum Dis. 2005; 64:1263–1267. [PubMed: 15731292]
39. Jackson MT, Moradi B, Zaki S, Smith MM, McCracken S, Smith SM, et al. Depletion of protease-activated receptor 2 but not protease-activated receptor 1 may confer protection against osteoarthritis in mice through extracartilaginous mechanisms. Arthritis Rheumatol. 2014; 66:3337–3348. [PubMed: 25200274]
40. Morand EF, Bucala R, Leech M. Macrophage migration inhibitory factor: an emerging therapeutic target in rheumatoid arthritis. Arthritis Rheumatol. 2003; 48:291–299.
41. Kuhn K, D'Lima DD, Hashimoto S, Lotz M. Cell death in cartilage. Osteoarthritis Cartilage. 2004; 12:1–16. [PubMed: 14697678]
42. Mun SH, Oh D, Lee SK. Macrophage migration inhibitory factor down-regulates the RANKL-RANK signaling pathway by activating Lyn tyrosine kinase in mouse models. Arthritis Rheumatol. 2014; 66:2482–2493. [PubMed: 24891319]
43. Dequeker J, Aerssens J, Luyten FP. Osteoarthritis and osteoporosis: clinical and research evidence of inverse relationship. Aging Clin Exp Res. 2003; 15:426–439. [PubMed: 14703009]
44. Zhang Y, Hannan MT, Chaisson CE, McAlindon TE, Evans SR, Aliabadi P, et al. Bone mineral density and risk of incident and progressive radiographic knee osteoarthritis in women: the Framingham Study. J Rheumatol. 2000; 27:1032–1037. [PubMed: 10782833]
45. Onodera S, Nishihira J, Iwabuchi K, Koyama Y, Yoshida K, Tanaka S, et al. Macrophage migration inhibitory factor up-regulates matrix metalloproteinase-9 and -13 in rat osteoblasts. Relevance to intracellular signaling pathways. J Biol Chem. 2002; 277:7865–7874. [PubMed: 11751895]
46. Kleemann R, Hausser A, Geiger G, Mischke R, Burger-Kentischer A, Flieger O, et al. Intracellular action of the cytokine MIF to modulate AP-1 activity and the cell cycle through Jab1. Nature. 2000; 408:211–216. [PubMed: 11089976]
47. Cross M, Smith E, Hoy D, Nolte S, Ackerman I, Fransen M, et al. The global burden of hip and knee osteoarthritis: estimates from the global burden of disease 2010 study. Ann Rheum Dis. 2014; 73:1323–1330. [PubMed: 24553908]
48. Bucala R. MIF, MIF alleles, and prospects for therapeutic intervention in autoimmunity. J Clin Immunol. 2013; 33(Suppl 1):S72–78. [PubMed: 22968741]

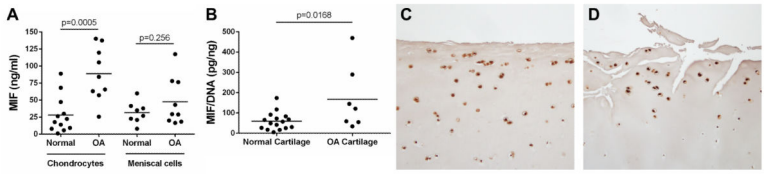

Figure 1.

MIF levels in conditioned media from normal and OA chondrocyte and meniscal cell cultures and in normal and OA cartilage sections. **A.** Serum-free medium was collected after 16 hours of culture from unstimulated confluent monolayers of normal and OA chondrocytes and meniscal cells. MIF protein in media was measured by human MIF ELISA. Horizontal lines on the graph represent average MIF level for each tissue type; individual data points are shown. Normal chondrocytes: n=12 donors; OA chondrocytes: n=9 donors; normal meniscus: n=8 donors; OA meniscus: n=9 donors. Statistical significance was evaluated by unpaired t-test within tissue types. **B.** Serum-free conditioned medium was collected after 48 hours of culture from unstimulated human and OA cartilage explants. MIF protein in media was measured by human MIF ELISA and was normalized to the DNA content of the explants. Individual data points are shown. Normal cartilage explants: n=16 donors; OA cartilage explants: n=7 donors. Statistical significance was evaluated by unpaired t-test, and no outliers were identified by the Grubbs outlier test. Immunohistochemistry results for MIF in sections of **(C)** human normal knee cartilage and **(D)** human OA knee cartilage.

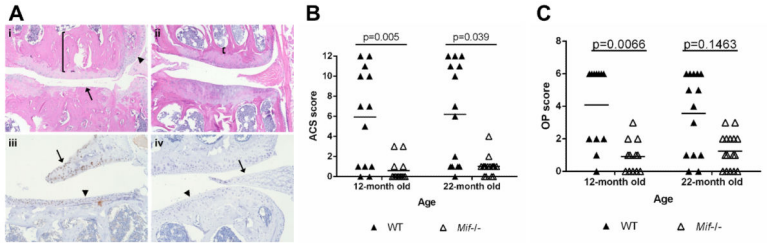

Figure 2.

Mice with *Mif* deletion are protected from age-related OA. **A.** Representative histologic images of knee joint sections in 12-month old *Mif*−/− and WT mice. (i) WT mouse, medial tibial plateau (MTP) articular cartilage structure (ACS) score 11. Degradation and loss of articular cartilage (arrow), osteophyte formation (arrowhead), and thickening of subchondral bone (bracket). (H&E) (ii) *Mif*−/− mouse, ACS score 3. Normal subchondral bone thickness (bracket). (H&E) (iii) WT mouse section immunostained for MIF. Intracellular MIF is present in meniscus (arrow) and articular cartilage (arrowhead). (iv) *Mif*−/− mouse. Lack of MIF immunopositivity in meniscus (arrow) and cartilage (arrowhead). **B.** Articular cartilage structure scores in *Mif*−/− and WT mice. The medial tibial plateau of mid-coronal stifle sections was scored using the articular cartilage structure (ACS) score. 12-month old WT: n=13; 12-month old *Mif*−/−: n=13; 22-month old WT: n=14; 22-month old *Mif*−/−: n=16. **C.** Osteophyte scores in *Mif*−/− and WT mice from (**B**). The summed scores from the medial tibial plateau (MTP) and medial femoral condyle (MFC) are presented. Horizontal lines on graph represent the mean of each group. Significant differences were determined by Kruskal-Wallis nonparametric one-way ANOVA followed by Dunn's multiple comparisons test.

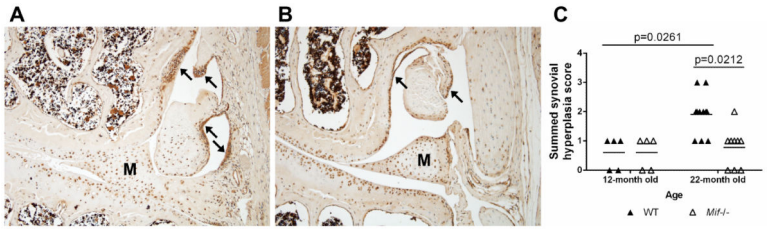

Figure 3.

Synovial hyperplasia is less severe in 22-month old mice with *Mif* deletion. Immunohistochemistry results for S100A8 in **(A)** 22-month old WT mouse, ACS score 11, and **(B)** 22-month old *Mif*−/− mouse, ACS score 0. Arrows indicate regions of strong synovial S100A8 immunopositivity and synovial hyperplasia. Representative histologic images are shown. M=meniscus. **C.** Synovial hyperplasia scores of the medial and lateral compartments were summed from 12-month old WT (n=5) and *Mif*−/− (n=5) and from 22-month old WT (n=11) and *Mif*−/− (n=9) mice. Horizontal lines on graph represent the mean of each group. Significant differences were determined by Kruskal-Wallis nonparametric one-way ANOVA followed by Dunn's multiple comparisons test.

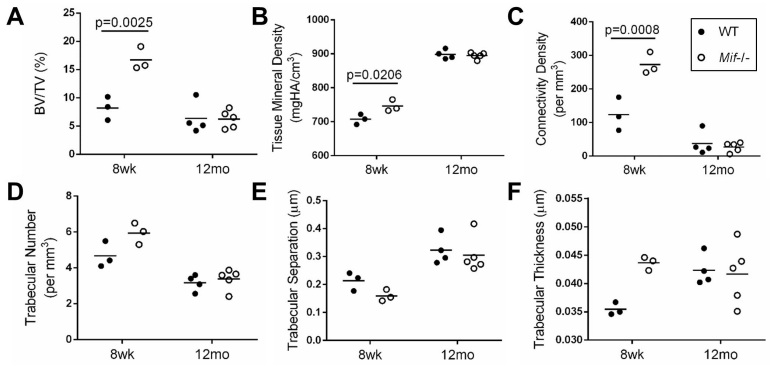

Figure 4.

µCT analysis of 8-week old and 12-month old male mice with *Mif* deletion and wild-type controls. Bone density parameters of the proximal metaphysis of the tibia were analyzed using Scanco software in 8-week old WT (n=3) and *Mif*−/− (n=3) and in 12-month old WT (n=4) and *Mif*−/− (n=5) mice. **A.** Bone volume fraction. (BV/TV=bone volume/total volume) **B.** Tissue mineral density. (HA=hydroxyapatite) **C.** Connectivity density. **D.** Trabecular number. **E.** Trabecular separation. **F.** Trabecular thickness. Horizontal lines on graphs represent the mean of each group. Significant differences were determined by two-way ANOVA followed by Tukey's multiple comparisons post-hoc test.

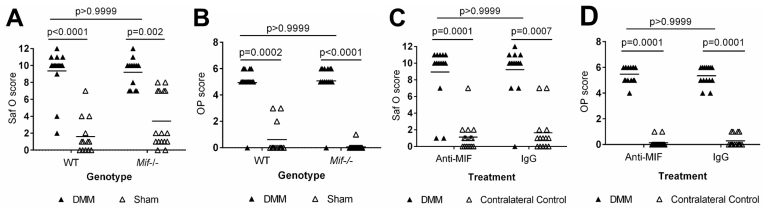

Figure 5.

Inhibition of MIF activity either by gene deletion or by neutralizing antibody does not protect young adult mice from injury-induced OA. **A.** Twelve-week old *Mif*−/− or WT mice received either the DMM or sham procedure. OA severity was analyzed 10 weeks after surgery by the Saf-o score. *Mif*−/− DMM: n=14; *Mif*−/− sham: n=16; WT DMM: n=16; WT sham: n=13. **B.** Osteophytes were measured in the mice from (**A**) and summed scores from the MTP and MFC are presented. **C.** Twelve-week old WT mice received the DMM procedure and were treated for 10 weeks with either the MIF neutralizing antibody (Anti-MIF) or IgG control antibody. The contralateral limb was used as the un-operated control. OA severity was analyzed 10 weeks after surgery by the Saf-O score. Anti-MIF DMM: n=15; Anti-MIF contralateral control: n=15; IgG DMM: n=14; IgG contralateral control: n=14. **D.** Osteophytes were measured in the mice from (**C**) and summed scores from the MTP and MFC are presented. Horizontal lines on the graph represent the mean of each group. Significant differences were determined by Kruskal-Wallis nonparametric one-way ANOVA followed by Dunn's multiple comparisons test.

Table 1

Histomorphometric analysis of aged mice with *Mif* deletion and wild-type controls.

	12-month old			22-month old			WT 12- vs 22-month olds
Parameter	***Mif*−/− Mean (SD)**	**WT Mean (SD)**	**p-value**	***Mif*−/− Mean (SD)**	**WT Mean (SD)**	**p-value**	**p-value**
Art Cart Area (mm^2)	0.064 (0.011)	0.040 (0.016)	<0.001	0.064 (0.008)	0.029 (0.018)	<0.001	.089
Art Cart Thickness (mm)	0.072 (0.013)	0.043 (0.017)	<0.001	0.078 (0.009)	0.037 (0.019)	<0.001	.339
Subchondral Bone Area (mm^2)	0.080 (0.016)	0.156 (0.069)	0.002	0.070 (0.025)	0.103 (0.038)	0.009	.024
Subchondral Bone Thickness (mm)	0.059 (0.011)	0.104 (0.046)	0.004	0.070 (0.023)	0.100 (0.037)	0.013	.772
Number of Viable Chondrocytes	138.39 (16.15)	74.31 (41.38)	<0.001	115.50 (21.98)	64.14 (45.24)	0.001	.549
Area of chondrocyte necrosis (mm^2)	0.008 (0.006)	0.006 (0.004)	0.396	0.008 (0.011)	0.007 (0.008)	0.859	0.602
Calcified cartilage area (mm^2)	0.063 (0.012)	0.059 (0.019)	0.504	0.049 (0.005)	0.053 (0.019)	0.368	.421

Histomorphometry measurements of cartilage (Cart) and bone parameters in the medial tibial compartment of mid-coronal stifle sections were analyzed using the Osteomeasure Histomorphometry Program (OsteoMetrics®). 12-month old WT: n=13; 12-month old *Mif*−/−: n=13; 22-month old wild-type (WT): n=14; 22-month old *Mif*−/−: n=16. Significance differences determined by heteroscedastic t-test using SPSS.